

beech was first established at White Pond, South Carolina, at 12,800 years B.P. (3), slightly later at Singletary Lake, North Carolina (2), and more than 1000 years later in an attenuated form at Rockyhook Bay, North Carolina (2). Species-diverse deciduous forest is not recorded at Lake Annie (4).

3) The Holocene began about 12,000 years ago with the decline of mesic forest and the rise of pine and oak to dominance in the landscape.

W. A. WATTS

Department of Botany, Trinity College, Dublin 2, Ireland, and Limnological Research Center, University of Minnesota, Minneapolis 55455

M. STUIVER

Quaternary Research Center, University of Washington, Seattle 98195

References and Notes

1. CLIMAP = Climate: Long-Range Investigation, Mapping, and Prediction. See A. D. Hecht, R. Barry, H. Fritts, J. Imbrie, J. Kutzbach, J. Mitchell, S. M. Saven, *Quat. Res. (N.Y.)* **12**, 6 (1979); G. M. Peterson, T. Webb III, J. E. Kutzbach, T. Van Der Hammen, T. A. Wijmstra, F. A. Street, *ibid.*, p. 47; S. Manabe and D. G. Hahn, *J. Geophys. Res.* **82**, 3889 (1977).
2. Singletary Lake: D. R. Whitehead, *Quaternary Paleogeology*, E. J. Cushing and H. E. Wright, Jr., Eds. (Yale Univ. Press, New Haven, Conn., 1967), p. 237. Rockyhook Bay: D. R. Whitehead, *Quat. Res. (N.Y.)* **3**, 621 (1973). Bob Black Pond: W. A. Watts, *Ecology* **51**, 17 (1970).
3. W. A. Watts, *Quat. Res. (N.Y.)* **13**, 187 (1980).
4. _____, *Geology* **3**, 344 (1975).
5. E. C. Pirkle and H. K. Brooks, *J. Geol.* **67**, 302 (1959).
6. Mud Lake: W. A. Watts, *Geol. Soc. Am. Bull.* **80**, 631 (1969). Lake Louise: _____, *Ecology* **52**, 676 (1971).
7. C. J. Clausen, A. D. Cohen, C. Emiliani, J. A. Holman, J. J. Stipp, *Science* **203**, 609 (1979).
8. Named on Gold Head Branch topographic map of the U.S. Geological Survey (water depth, 18 m).
9. N. L. Christensen, in "U.S. Forest Service General Technical Report," H. Mooney *et al.*, Eds. (Forest Service, Department of Agriculture, Washington D.C., in press).
10. A. M. Laessle, *Ecol. Monogr.* **28**, 361 (1958).
11. "Mesic trees" are the sum of ironwood (*Ostrya Carpinus*), elm (*Ulmus*), ash (*Fraxinus*), beech (*Fagus*), sugar maple (*Acer saccharum*), and basswood (*Tilia*). Papillate pollen grains of cypress (*Taxodium*) identify the genus. As no papillate grains occur, *Taxodium* was probably absent during zone Sh-2 and early zone Sh-3. "Juniper type" includes burst pollen grains of *Taxodium* and pollen of southern red cedar (*Juniperus silicicola*) and white cedar (*Chamaecyparis thyoides*). Southern red cedar is widespread locally at present, but isolated stands of white cedar occur near Sheelar Lake (13). "Swamp trees and shrubs" include wax myrtle (*Myrica*), dahoon (*Ilex*), loblolly bay (*Gordonia*), and Virginia willow (*Itea*). "Upland herbs" include Gramineae, Cyperaceae, *Selaginella arenicola*, *Polygonella* spp., *Rumex*, *Chenopodium* type, *Ambrosia*, Tubuliflorae, *Iva*, *Artemisia*, *Amorpha*, Umbelliferae, and others.
12. T. Webb III, *Ecology* **55**, 17 (1974).
13. E. L. Little, Jr., *Atlas of United States Trees*, vol. 5, *Florida* (Miscellaneous Publication 1361, Forest Service, Department of Agriculture, Washington D.C., 1978).
14. D. B. Ward, *Rhodora* **69**, 51 (1967).
15. Anderson Pond: H. R. Delcourt, *Ecol. Monogr.* **49**, 255 (1979).
16. This research was supported by NSF grants BMS 75-04999 and DEB 77-20803 to the University of Minnesota. Contribution 157 of Limnological Research Center, University of Minnesota.

25 February 1980; revised 18 June 1980

steady state, fluid filtration is dependent mainly on the microvascular hydrostatic pressure; the term microvascular indicates our uncertainty about the actual pressure and proportion of total fluid exchange in various segments of the microcirculation.

Current knowledge of the microvascular pressure in the lung is derived from indirect measurements in isolated perfused dog lungs; such measurements yield only lumped values for the inflow and outflow segments. Using the low viscosity bolus-ether evolution technique, Brody *et al.* (4) estimated the longitudinal distribution of vascular resistance as being 46 percent arterial, 34 percent capillary, and 20 percent venous. Gaar *et al.* (5), using the isogravimetric pressure technique, measured the capillary hydrostatic pressure at the point of zero net filtration. They found that 56 percent of the total vascular resistance lay upstream of this point. These measurements form the basis of current estimates of microvascular pressure in zone III of the lung (where pulmonary venous pressure exceeds alveolar pressure). A hypothetical microvascular pressure is calculated on the premise that 60 and 40 percent of the total resistance lie in the arterial and venous segments, respectively (6).

The relatively wide alveolar wall capillaries lying just under the pleural surface are easily visualized (7), but are not easy to puncture. There are several impediments. (i) The visceral pleura is surprisingly resistant to puncture, even in animals with thin pleuras, and micropipette tips are easily broken. (ii) With reflected light, optical illusions are created by the curved air-liquid interface of the alveoli. Vessels that seem to lie close to the surface often lie deeper and are inaccessible. What appears to be a ring of capillaries around the alveoli is often not. (iii) Motion of the lung surface resulting from ventilation or from cardiac and vascular pulsations increases the difficulty of micropuncture.

To avoid interference from vascular and ventilatory motion, we removed the left lower lobes [unperfused weight, 43.2 ± 1.3 g (standard deviation)] from

Direct Measurement of Microvascular Pressures in the Isolated Perfused Dog Lung

Abstract. *Microvascular pressures in the pulmonary circulation were measured under the pleural surface of the isolated perfused dog lung by the servo-null technique. Strong glass micropipettes with short beveled tips were used, with a suction ring to stabilize the lung's surface. Of the total vascular resistance, 45 percent was in the alveolar wall capillaries themselves. Most of the remaining resistance was in the arterioles. There was negligible pressure drop in venules with diameters larger than 20 micrometers.*

Although microvascular pressure has been measured by capillary micropuncture in several organs (1), such measurements have not succeeded in the lung (2). We now report direct measurements of microvascular pressure in the lung.

Net transvascular fluid filtration in the lung, as in other organs, is dependent on the differences in hydrostatic and osmotic pressures across the microvascular endothelial barrier, as described in the modified Starling equation (3). In the

Table 1. Direct pressure measurement in blood vessels of the isolated perfused dog lung. Pressures are given as means \pm standard deviation.

Measure	Arteries			Capillaries			Veins	
	Pulmonary artery	30 to 50 μ m	20 μ m	10 μ m, arterial	10 μ m, venous	20 μ m	30 to 50 μ m	Pulmonary vein
Pressure (cm-H ₂ O)	16.7 \pm 0.6	16.4 \pm 1.3	15.6 \pm 2.9*	14.6 \pm 2.4*	12 \pm 1.7*	11.1 \pm 0.7*	11.1 \pm 0.8	11.1 \pm 0.5
Number of vessels	10	7	3	13	10	4	8	10
Percent of total resistance		5.4	14.2	17.9	46.4	16.1	0	0

*Values are significantly different from those in previous column at $P < .05$ (Newman-Keuls test).

anesthetized dogs and perfused them with a nonpulsatile flow of autologous heparinized blood at 38°C and constant pressure. We set the inflow (pulmonary arterial) and outflow (pulmonary venous) pressures (Table 1) to give a reasonable blood flow (5.2 ± 1.1 ml/g-min) and to be above alveolar pressure so as to congest the lobe (zone III). This maintained the capillaries in their distended oval cross section and aided visualization. We could not completely overcome the optical illusion at the lobe surface; that required experience as well as trial and error.

To avoid excessive stretch of the microvessels and to stabilize the lung surface, we held alveolar pressure constant at 5 cm-H₂O with 50 percent O₂ and used a suction ring, modified from one devised by Wagner and Latham (7), to grip the lung surface.

To overcome pleural resistance to micropuncture, we constructed short-tipped beveled glass micropipettes that were both rigid and strong. Our micropipettes (8) had tip diameters of 2 to 3 μm, tip lengths not exceeding 300 μm, and tip impedances of 2 to 5 megohms.

We made measurements with a Wiederhielm-type servo-null pressure measuring device, which provides measurements that are stable, reproducible, and accurate (9). We lowered the micropipette, filled with 2M NaCl colored with green dye, onto a target vessel, so that flow in the vessel was momentarily interrupted by pressure from the pipette tip. This confirmed the accessibility of the vessel. With a quick forward motion of the pipette, we punctured the vessel.

We tested the validity of the recorded pressure by requiring that two of the following criteria be met: (i) tight coupling of recorded microvascular pressure to induced fluctuations in pulmonary arterial or venous pressure, (ii) rapid washout of dye injected through the micropipette, (iii) high-frequency oscillation of the servo-null system at high gain. The last condition is met only if the micropipette lies in free fluid.

With these criteria, we have a 20 percent success rate. The arteries and veins are easily identified on the lung's surface by the direction of flow; for instance, in an arterial vessel, the flow is into smaller vessels. The branching pattern is fairly distinct. Arterioles, 30 to 50 μm in diameter, branch abruptly, giving rise to 20-μm arterioles that in turn give off 10-μm arterial capillaries. Some capillaries arise directly from larger arterioles. On the venous side, the 10-μm capillaries join into 20-μm venules, which coalesce into larger ones. In the subpleural region of

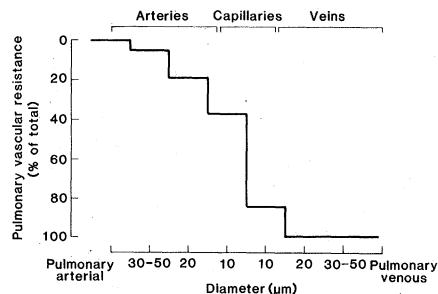


Fig. 1. Profile of distribution of vascular resistance along the circulation in the isolated perfused dog lung lobe in zone III. Since flows in each longitudinal segment are equal, the ordinate is also the fractional drop in pressure. The greatest resistance lies between the arterial and venous capillaries. There is little resistance upstream of the 50-μm arterioles on the inflow side or in veins larger than 20 μm on the outflow side.

the lung there are many more venous than arterial vessels (10).

Microvascular pressures from 45 vessels in ten lobes are summarized in Table 1. The arterial-venous pressure difference was not large, but allowed blood flows of more than 200 ml/min for 3 to 4 hours without the development of alveolar edema in the lobes. Because we have found that the total vascular resistance in these lobes remains unchanged for 4 hours (11), we made all pressure measurements within this period. We could not prevent interstitial edema, since we held venous pressure approximately 6 cm-H₂O above alveolar pressure to distend the capillaries. The recorded pressure in all microvessels was substantially above isogravimetric pressure measured under roughly similar conditions (12).

The fractional resistance along the various segments of the lobe circulation (Fig. 1) is equivalent to the fractional pressure drop because total lobar blood flow was the same through all vascular segments. The data show little arterial resistance proximal to the 50-μm arterioles and no measurable venous resistance distal to the 20-μm venules. Thus we were unable to confirm the existence of a significant resistance in the large veins, reported in amphibian lungs and perfused dog lungs (2, 13). The largest pressure drop occurred between the arterial and venous capillaries. In the systemic circulation the greatest pressure drop occurs proximal to the capillary bed (14).

If the arterial and venous capillary pressures (Table 1) are averaged to obtain what might be the hydrostatic pressure at the midpoint of the pulmonary capillary network, 61 percent of the total resistance lies proximal to this capillary midpoint. This finding agrees well with

indirect estimates of resistance distribution (4, 5). In fact, our findings on resistance distribution so closely match those of Gaar (5), who measured isogravimetric pressure, that we speculate that the zero filtration point (their "effective" midpoint for fluid exchange) and the anatomic capillary midpoint coincide.

We believe that the pressures we have recorded in subpleural vessels probably represent pressures in similar vessels deep in the lung (10, 12), although there is no way at present to get at the deeper vessels. These measurements in the isolated lung may reflect corresponding values in the intact lung, but measurements in intact lungs have not been made. On the basis of our experience with isolated lobes, we believe it is feasible to make direct micropuncture measurements in the lungs of living animals.

J. BHATTACHARYA

N. C. STAUB

Cardiovascular Research Institute and
Department of Physiology, University
of California, San Francisco 94143

References and Notes

1. For example, (brain) D. D. Stromberg and H. Shapiro, *Microvasc. Res.* **5**, 410 (1973); (kidney) B. M. Brenner, J. C. Troy, T. M. Daugharty, *J. Clin. Invest.* **50**, 1776 (1971); (muscle) H. G. Bohlen, R. W. Gore, P. M. Hutchins, *Microvasc. Res.* **13**, 125 (1977).
2. J. E. Maloney and B. L. Castle, *Respir. Physiol.* **10**, 51 (1970).
3. The Starling equation for capillary fluid transport is

$$\dot{Q} = K[(P_{mv} - P_{pmv}) - \sigma(\pi_{mv} - \pi_{pmv})]$$
 where \dot{Q} is the net microvascular fluid flow (ml/min); K is the filtration coefficient (ml/min-cm-H₂O); P_{mv} is capillary hydrostatic pressure (cm-H₂O); P_{pmv} is perimicrovascular hydrostatic pressure (cm-H₂O); π_{mv} is plasma protein osmotic pressure (cm-H₂O); π_{pmv} is perimicrovascular protein osmotic pressure (cm-H₂O); and σ is the reflection coefficient.
4. J. S. Brody, E. J. Stemmler, A. DuBois, *J. Clin. Invest.* **47**, 783 (1968).
5. K. A. Gaar, A. E. Taylor, L. J. Owens, A. C. Guyton, *Am. J. Physiol.* **213**, 910 (1967). Isogravimetric pressure is the hydrostatic pressure in microvessels where filtration equals reabsorption; it is experimentally determined as the vascular pressure at zero flow in a lung at constant weight.
6. A. J. Erdmann, T. R. Vaughan, K. L. Brigham, W. C. Woolverton, N. C. Staub, *Circ. Res.* **37**, 271 (1975).
7. W. W. Wagner and L. P. Latham, *J. Appl. Physiol.* **39**, 900 (1975). The pressure in the suction ring was -5 cm-H₂O and the central opening in the ring, where we made our punctures, was 2 cm in diameter.
8. Kimble standard glass, No. 46485; pipette puller model 700c, David Kopf Instruments, Tujunga, Calif; beveler manufactured at the machine shop, Department of Physiology, University of Calif., San Francisco.
9. Model 4A, Instrumentation for Medicine, San Diego, Calif. [see C. A. Wiederhielm, *Methods Med. Res.* **11**, 199 (1966)].
10. N. C. Staub and E. L. Schultz, *Respir. Physiol.* **5**, 371 (1968).
11. J. Bhattacharya, K. Nakahara, N. C. Staub, *J. Appl. Physiol.* **48**, 444 (1980).
12. P. D. Snashall, K. Nakahara, N. C. Staub, *ibid.* **46**, 1003 (1979).
13. P. J. Kadowitz, P. D. Joiner, A. L. Hyman, *J. Clin. Invest.* **56**, 354 (1975); I. McDonald and J. Butler, *J. Appl. Physiol.* **23**, (1967).
14. E. M. Landis, *Am. J. Physiol.* **93**, 353 (1930).
15. Supported in part by National Heart, Lung, and Blood Institute program project grant HL06285.

28 January 1980; revised 24 June 1980